Prediction of Transition Due to Isolated Roughness

Tuncer Cebeci* and David A. Egan†
California State University, Long Beach, California

A combination of an interactive boundary-layer procedure and e^n-method has been used to determine the locations of the onset of transition for flows over a flat plate with bumps or hollows. The details of the procedure are examined and the need for fine-grid calculations in regions of strong adverse pressure gradients emphasized. The location of initial disturbance is shown to be unimportant, provided it does not occur in the region where the critical Reynolds number is higher than the flow Reynolds number. The procedure allows good results for flows with and without separation. Possible means of improvement of the method are discussed.

I. Introduction

THERE are many flow problems in which it is desirable or necessary to maintain extensive regions of laminar flow.[1,2] Granting that such a flow be attained, however, the first requirement is that the surface should be smooth so as not to affect the stability of the boundary layer. It is, therefore, of great importance to obtain an estimate of the maximum degree of surface roughness that can be tolerated without affecting transition.

The transition process is known to involve the growth of disturbances and the formation and destruction of Tollmien-Schlichting waves as demonstrated, for example, by Gaster.[3] It is complicated and unlikely to be represented in all respects in the forseeable future. On the other hand, available empirical equations such as those of Fage[4] and Carmichael[5-7] take no direct account of factors that are known to affect the process, including surface quality, turbulence intensity, and scale. A more soundly based approach is linear stability theory, which involves the solution of the Orr-Sommerfeld equation and the examination of the amplification rates of disturbances in the e^n-method proposed by Smith[8] and Van Ingen.[9] It is more complicated to use but, as the survey paper of Wazzan[10] shows, it can provide predictions of the onset of transition of wall boundary layers that are within the uncertainty of corresponding measurements.

The present paper describes a general method for calculating transition in separating and reattaching flows and applies the procedure to study the effect of isolated roughness, which can produce a flow with local separation on transition. The roughness shapes correspond to those of Fage[4] who studied the effects of bulges, hollows, and ridges on an airfoil and on a flat plate experimentally, and developed empirical relations between minimum roughness height, roughness width, and transition Reynolds number. The method is based on a combination of interactive boundary-layer and linear stability theories, as described in Secs. II and III. In the former case, the boundary-layer equations are solved in inverse mode for a laminar flow in which the relation between the inviscid and viscous flows is obtained through the Hilbert integral. By changing the height of the roughness element, solutions are obtained for a range of separating and reattaching flows at specified Reynolds numbers. The linear stability theory then is used to analyze the stability properties of the computed velocity profiles at various locations on the plate with the computed amplification rates employed in the e^n-method to determine the location of transition. The choice of the disturbance frequency needed in the e^n-method and the manner in which it is used are considered in detail in Sec. IV. This is particularly important since the present flows involve rapid changes in flow properties and regions of flow separation that have not been subjected previously to close scrutiny. Nayfeh et al.[11] have reported one approach to this problem, and the effect of the detailed differences in implementation are examined. The resulting values of transition are presented in Sec. V and compared with the measurements of Fage.[4]

II. Interactive Boundary-Layer Procedure

The interactive boundary-layer procedure has been used extensively in the solution of problems involving flow separation. For example, it has been applied to a wide range of airfoils at angle of attack, to unsteady flows with separation, and to three-dimensional flows over wings. As a consequence, its convenience and accuracy have been established and detailed descriptions provided. The following paragraphs outline the procedure, and the reader is directed to Refs. 12–14 for further detail.

The general procedure involves the solution of inviscid flow equations, but in the case of present flows the freestream velocity was constant and was used as the initial external velocity boundary condition for the viscous flow equations. The steady two-dimensional boundary-layer equations for laminar flow were solved in transformed coordinates in inverse form by the box scheme of Keller with its Mechul-function formulation. Interaction between the inviscid flow and viscous flow was accomplished with a form of the Hilbert integral proposed by Veldman.[15] This coupling procedure closely resembles the well-known triple-deck theory described, for example, by Stewartson,[16] but is not restricted to laminar flows.

The present flows involve separation and, to avoid the corresponding numerical difficulties associated with the longitudinal convection term $u(\partial u/\partial x)$, the FLARE approximation suggested by Reyhner and Flügge-Lotz was employed. This implies that in the region of negative u-velocity the longitudinal convection term is neglected. This approximation is adequate provided that the region of separated flow is small.

III. Linear Stability and the e^n-Methods

The calculation of the onset of transition requires the evaluation of the integral

$$n = \int_{x_0}^{x} -\alpha_i \, dx \tag{1}$$

for a set of specified dimensional frequencies ω^*. Here, α_i represents the amplification rates determined from the solutions of the Orr-Sommerfeld equation

$$\phi^{iv} - 2\alpha^2\phi'' + \alpha^4\phi - iR(\alpha u - \omega)(\phi'' - \alpha^2\phi) + iR\alpha u''\phi = 0 \tag{2}$$

Presented as Paper 88-0139 at the AIAA 26th Aerospace Sciences Meeting, Reno, NV, Jan. 11–14, 1988; received Jan. 22, 1988; revision received May 13, 1988.

*Professor and Chairman, Department of Aerospace Engineering. Fellow AIAA.

†Graduate Student, Department of Aerospace Engineering.

Equation (2) has been written in dimensionless form so that all velocities and lengths are normalized by a reference velocity u_0 and length ℓ so that the Reynolds number R is defined by $R = u_0\ell/\nu$. The radian frequency ω is made dimensionless by dividing the physical frequency ω^* by u_0/ℓ. Primes denote differentiation with respect to a dimensionless distance $y(\equiv y/\ell)$. The wavelength α, which is complex ($\equiv \alpha_r + i\alpha_i$), also has been normalized by the reference length ℓ. In the present method, we use spatial amplification theory and, thus, assume that ω is real.

The solution of Eq. (2) requires that velocity profiles u and their second derivatives u'' be obtained from the interactive boundary-layer procedure of Sec. II. With this information, the solution reduces to an eigenvalue problem involving the four scalars α_r, α_i, R, and ω. The numerical procedure to solve this eigenvalue problem is described in Ref. 17. It is clear that the value of R is known at any streamwise station and that the real and imaginary parts of wave number α provide two equations. Thus, solutions can be obtained provided ω is known. One procedure for determining ω is described in the following section, and its consequences are examined and compared with those of the alternative approach of Ref. 11.

In the absence of surface disturbances, the flow of Fage is close to that of a flat plate laminar flow. In this case, the e^n-method leads to the calculation of amplification factors of Fig. 1. This result and means of achieving it provide a foundation for the more complex flows associated with surface irregularities considered in the following section.

With the velocity profiles obtained by solving the Blasius equation, the solution of Eq. (2) begins at a Reynolds number R greater than the critical value R_{cr}, which in this case is known to be 520 based on the displacement thickness R_{δ^*} on the lower branch of the neutral stability curve. This provides the desired frequency that at the subsequent Reynolds numbers allows the solution of the eigenvalue problem in which α is computed. This leads to one of the amplification curves of Fig. 1. The process is repeated to obtain similar amplification curves for different values of ω^*. As can be seen from Fig. 1, the envelope of the resulting curves corresponds to the maximum amplification factors from which transition is computed by assuming a value for n, commonly taken to be between 8 and 9.

This envelope procedure is useful and convenient for two-dimensional attached flows but has limitations for more complicated flows such as those with separation, as discussed in the following section. A more general method would require the determination of the first dimensional frequency, referred to as the critical frequency, which achieves the predetermined amplification factor corresponding to transition. For example, referring to Fig. 1, we observe that the amplification factor computed with $\omega^* = 885$ Hz has not achieved the desired amplification factor (say $n = 9$), and the appropriate value of ω^* is between 662 and 759 and needs to be determined accurately.

IV. Application of the Interactive Boundary Layer and e^n-Methods to Fage-Flows

The experiments of Fage were carried out with a flow configuration of a bump represented by the expression

$$\frac{y}{h} = \begin{cases} 1 - 12\left(\frac{x}{B}\right)^2 - 16\left(\frac{x}{B}\right)^3 & -\frac{B}{2} < x < 0 \\ 1 - 12\left(\frac{x}{B}\right)^2 + 16\left(\frac{x}{B}\right)^3 & 0 < x < \frac{B}{2} \end{cases} \tag{3}$$

where h and B denote the height and width of the bump. They involved a range of bump heights and Reynolds numbers at a distance of 20 in. from the leading edge of a flat plate with a bump width of 4 in. The interactive boundary-layer procedure was used to determine the characteristics of the laminar flows for the specified Reynolds number based upon the freestream velocity u_{1c} in the plane of the bump and distance from the leading edge. A sample of the results is shown in Fig. 2 and corresponds to the distributions of wall shear parameter f_w'' for

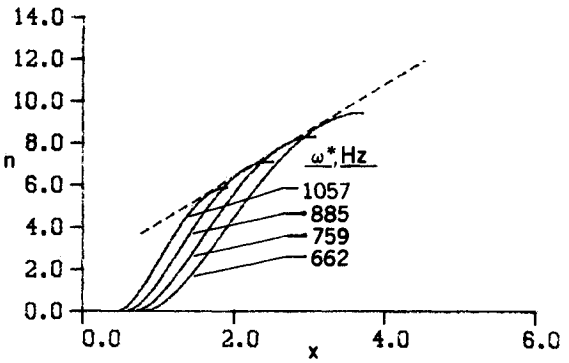

Fig. 1 Variation of the amplification factors with distance and frequency for a flat-plate flow.

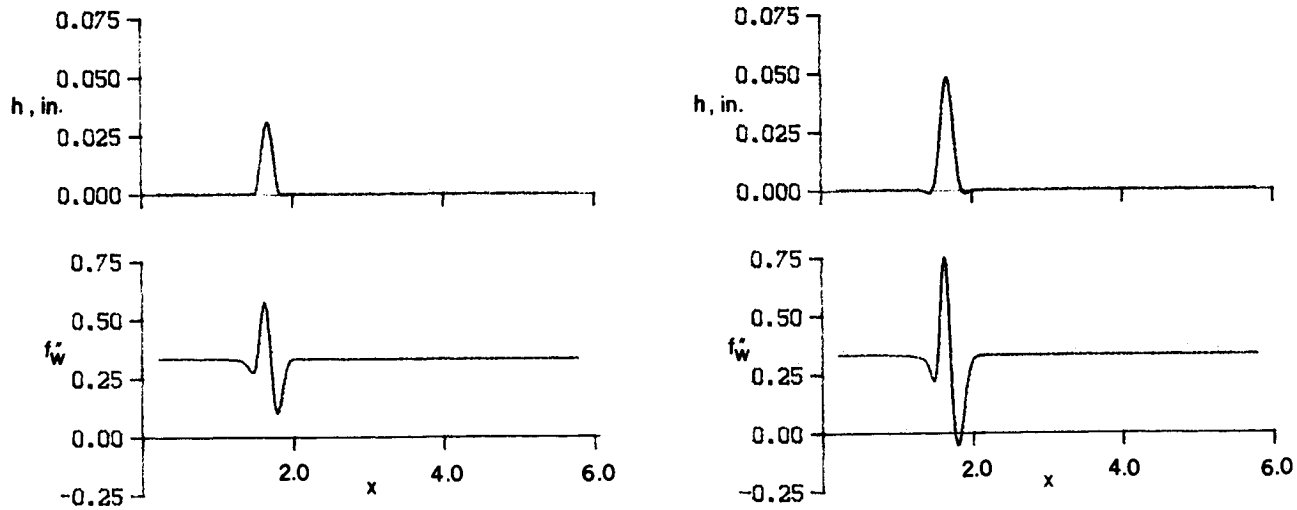

Fig. 2 Variation of the wall shear parameter f_w'' for two bump heights: a) $h = 0.0310$ in., b) $h = 0.0525$ in.

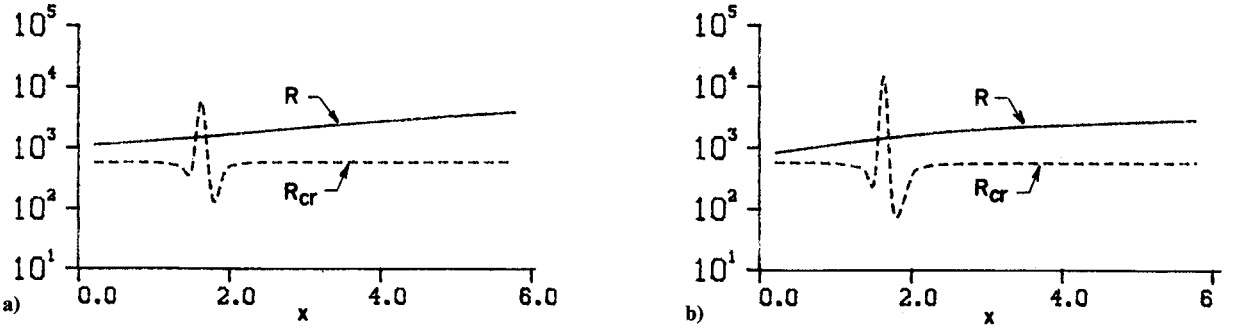

Fig. 3 Variation of the flow Reynolds number R ($\equiv u_e\delta^*/\nu$) and critical Reynolds number R_{cr} for the two bump heights of Fig. 2: a) $h = 0.0310$ in., b) $h = 0.0525$ in.

two bump heights h of 0.031 and 0.0525 in. and values of u_{1c} of 82.6 and 69.4 ft/s, respectively. Here, the wall shear parameter f_w'' is related to local skin-friction coefficient c_f by $f_w'' = c_f/2\sqrt{R_L}$ where the Reynolds number is defined in terms of u_0 and plate length L. As may be seen, the variations in wall shear parameter f_w'' are substantial, and the larger bump gives rise to a region of separated flow. These distributions and the corresponding velocity profiles are in marked contrast to the Blasius flow results that gave rise to Fig. 1.

It can be anticipated that the flow of Fig. 2 will pose problems for the application of the e^n-method. In particular, the rapid change from zero pressure gradient to a combination of strong favorable and adverse pressure gradients raises a question as to the appropriate Reynolds number with which to begin the stability calculations. It is not known a priori whether or not a disturbance initiated in the zero pressure gradient flow and allowed to amplify in the first region of adverse pressure gradient will be damped in the subsequent region of favorable pressure gradient. Similarly, if the disturbance grows in the region of adverse pressure gradient leading to separation, the rapid variations in the wall shear parameter f_w'' are likely to imply the need for careful control of numerical step lengths in the solution of the boundary-layer equations, the stability equation, and in the determination of the critical frequency.

To provide understanding of the influence of the Reynolds number used to initiate the stability calculations, results were obtained for a Reynolds number corresponding to a location well inside the region of zero pressure gradient upstream of the bumps. These results include distributions of critical Reynolds number R_{cr} and flow Reynolds number R as shown in Fig. 3. The values of R_{cr} are based on the solutions of the Falkner-Skan equation as demonstrated by Wazzan[10] and extended and included those with reverse flow by Wang[18] and are shown as a function of shape factor H in Fig. 4. It is evident that R_{cr} exceeds R in a small region of each flow so that the stability calculations on the lower branch of the neutral curve cannot be initiated in this region, although the present calculations (see Fig. 5) show that they can continue through this region from an upstream initial location with stability calculations not confined to the neutral curve.

Figure 5 shows the amplification factors for the flows of Figs. 2 and 3 and confirms that the effect of starting location is unimportant. In particular, a disturbance introduced upstream of the bump results in the same amplification factors as one introduced in the adverse pressure gradient region. It appears that the critical frequency determined in the zero pressure gradient region is the same as that found from the adverse pressure gradient region (see Fig. 6), and the amplification continues from the upstream region. This suggests that it is logical to seek the critical frequency in calculations begun in the adverse pressure gradient region.

Comparison of the amplification factors of Figs. 1 and 5 confirm that the effect of the strong adverse pressure gradient is to cause them to increase more rapidly. Where separation occurs, this increase extends to higher values and makes the identification of the transition location, corresponding to a particular value of n, more accurate.

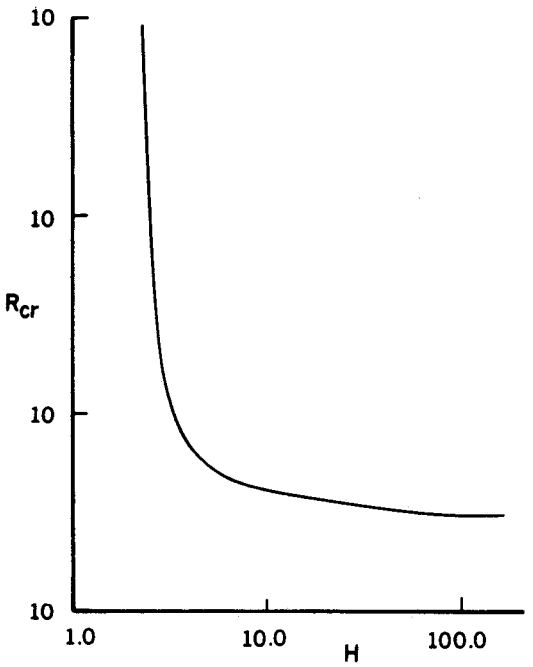

Fig. 4 Variation of the critical Reynolds number based on displacement thickness R_{cr} with shape factor H for Falkner-Skan flows.

In the region of steep adverse pressure gradient, it is found to be necessary to take small step lengths in Δx to allow the accurate determination of the critical frequency. Since the inverse method makes use of the Hilbert integral whose solutions exhibit a singularity as distance is reduced, the calculations are performed in two stages. In the first step, the solutions were obtained with a nonuniform grid with collocation points centered about the bump with spacing increasing in both directions in a geometrical progression. In the second step, a new and finer grid was generated by linearly dividing the region of interest and interpolating the values of displacement thickness, which served as a boundary condition for the final inverse calculations. The resulting velocity profiles were used in the stability analysis.

V. Calculated Values of Transition

The procedure described in the previous sections was used to determine the location of the onset of transition for the experimental configurations reported by Fage. It was assumed $n = 8.4$, a value that agrees with that obtained from the zero pressure gradient flow of Schubauer and Klebanoff.[20] Table 1 allows comparison of calculated and measured values for

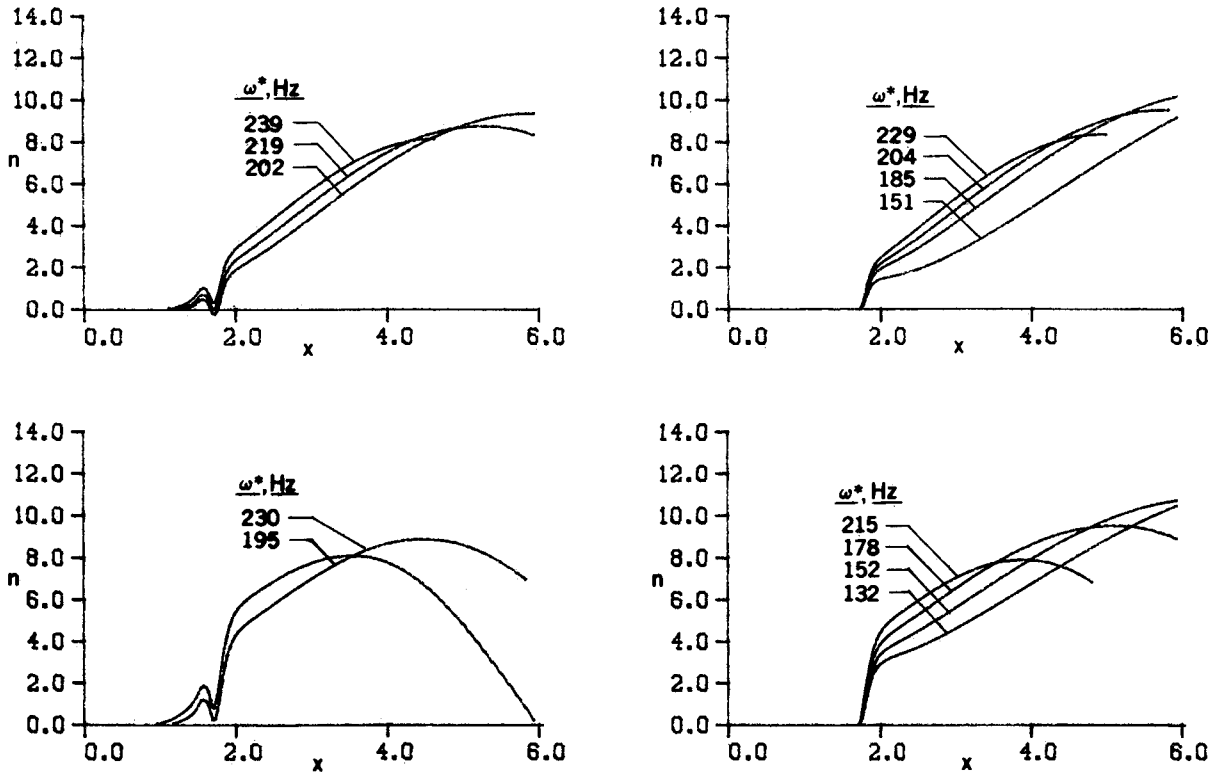

Fig. 5 Variation of the amplification factors with distance and frequency for the two bump heights of Fig. 3: a) $h = 0.0310$ in., b) $h = 0.0525$ in.

Table 1 Calculated and measured values of the location of transition, L_{tr} and $(L_{tr}/h)^{-1}$ for $n = 8.4$

			L_{tr}, ft		$(L_{tr}/h)^{-1}$		
Smooth bulge u_{1c}, ft/s	h, in.	f_{cr}, Hz	Exp	e^n	Exp	e^n	Fage correlation
			$\Lambda_x = 1.35$				
70.4	0.0555	236	4.58	2.95	0.00101	0.00157	0.00120
56.2	0.0665	146	4.58	3.41	0.00121	0.00163	0.00123
53.8	0.0700	128	4.58	3.47	0.00127	0.00168	0.00128
76.0	0.0555	257	3.75	2.67	0.00123	0.00173	0.00135
62.4	0.0630	171	3.75	3.20	0.00140	0.00164	0.00129
55.5	0.0680	139	3.75	3.43	0.00151	0.00165	0.00126
			$\Lambda_x = 0.90$				
82.6	0.0310	204	4.58	4.53	0.00056	0.00057	0.00048
69.4	0.0525	178	4.58	3.85	0.00096	0.00114	0.00105
53.0	0.0620	124	4.58	4.45	0.00113	0.00116	0.00098
78.0	0.0530	301	3.75	2.72	0.00118	0.00162	0.00128
61.5	0.0620	189	3.75	3.30	0.00138	0.00157	0.00122
95.0	0.0525	373	2.92	2.10	0.00150	0.00208	0.00169
70.0	0.0620	207	2.92	2.96	0.00177	0.00175	0.00149
92.4	0.0620	267	2.08	2.48	0.00248	0.00208	0.00226
			$\Lambda_x = 1.35$				
65.8	0.067	190	4.58	3.70	0.00122	0.00151	0.00158
76.4	0.057	251	4.58	3.36	0.00104	0.00141	0.00143
61.9	0.067	168	3.75	4.08	0.00149	0.00137	0.00144
82.7	0.057	321	3.75	2.83	0.00127	0.00168	0.00161
69.7	0.067	227	2.92	3.25	0.00191	0.00172	0.00173
84.9	0.057	353	2.92	2.67	0.00163	0.00178	0.00168

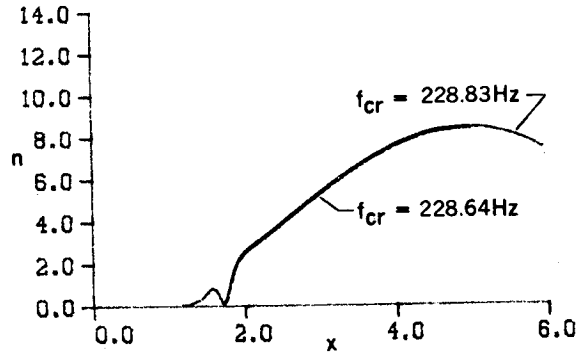

Fig. 6 Variation of the amplification factors with distance at two critical frequencies f_{cr} = 228.83 and 228.64 Hz computed in the favorable and adverse pressure gradient regions, respectively.

bumps and hollows. It should be recognized that these measurements were obtained from total head pressures and are subject to some uncertainty. Also, the calculations assumed zero pressure gradient, whereas the experiments suggest that the pressure gradient was slightly favorable close to the leading edge. An estimate of the strength of this pressure gradient was made in terms of the Falkner-Skan parameter β ($u_e = Cx^{\beta/2-\beta}$). It revealed a value of around 0.06 for the smooth bump for which Λ_x ($= \delta^2/\nu\ du_e/dx$) = 0.90 and a value of 0.093 for Λ_x = 1.35. The consequences of this pressure gradient is to suppress the disturbance growth and will cause the measured transition location to occur further downstream, particularly for those smaller bumps that result in separation. When there is no separation, the effect of the bumps on the transition process is reduced, and the less severe adverse pressure gradient has only a small effect on the growth of disturbances. This explains in part the good agreement between the present results and those of Nayfeh et al.[11] for the nonseparated flow u_{1c} = 82.6 ft/s, h = 0.0310 in. It is useful to note that their calculations for bump flows with separation tend to show transition locations consistently further upstream than those of the experiment, due in part to their choice of a critical frequency based on the Blasius flow and evaluated from $f_{cr} = 25 \times 10^6\ (u_\infty^2/\nu)(1/2\pi)$ Hz.

The results shown in the table are in general agreement with measurements as well as Fage's correlation, with a tendency for the calculated values of transition by the e^n-method to occur upstream of the measured values. The maximum discrepancy is of the order of 30% of the distance from the leading edge, and the average discrepancy is of the order of 17%. Part of these discrepancies is due to the favorable pressure gradient which, if included in the calculations, would move the computed transition locations downstream of the values shown. Some uncertainty also must be attributed to the experiments. It remains also to determine the influence of the shape of the bumps that have been approximated by Eq. (3) and to examine the inaccuracy caused by the FLARE approximation used in separated flows. In this last connection, it is known that the addition of the longitudinal convection term can influence results for the larger regions of separation.

Calculations have been performed for bump heights larger than those examined by Fage. Results for values of h of 0.092 in. and 0.10 in. are shown in Figs. 7 and 8. It is evident that the location of transition has moved upstream with bump height until, at the value of h = 0.10 in. shown in Fig. 8, it occurs inside the separation bubble. In this case there is no doubt that a calculation procedure with this location of transition and subsequent turbulent-flow assumptions would influence the upstream flow characteristics and those of the bubble itself. A similar conclusion is appropriate to the other bump heights that result in transition at a short distance downstream of the separation bubble. The resolution of this uncertainty

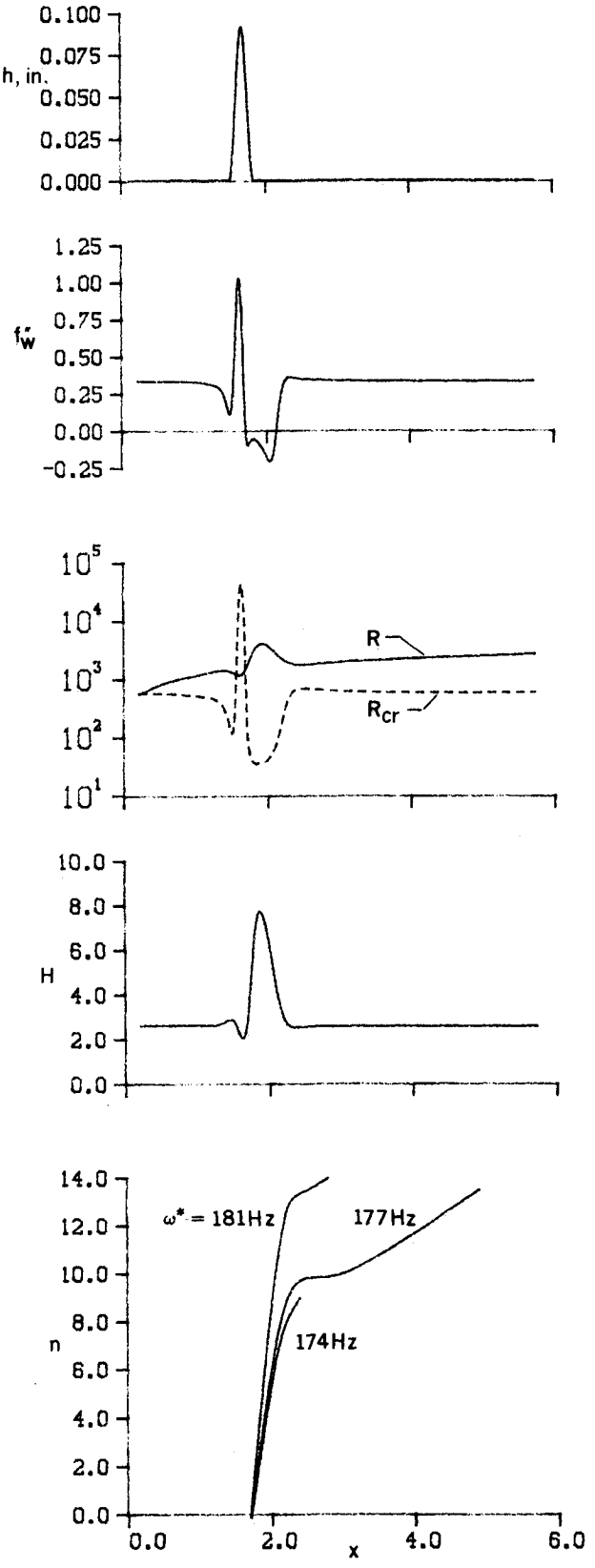

Fig. 7 Computed results for h = 0.092 in.

requires the use of an interactive boundary-layer procedure with a model for the transitional and turbulent flow and iterative calculations until a converged value of the transition location is obtained. Similar deductions have been made by Cebeci[19] in relation to steady separation bubbles on airfoils at low Reynolds numbers.

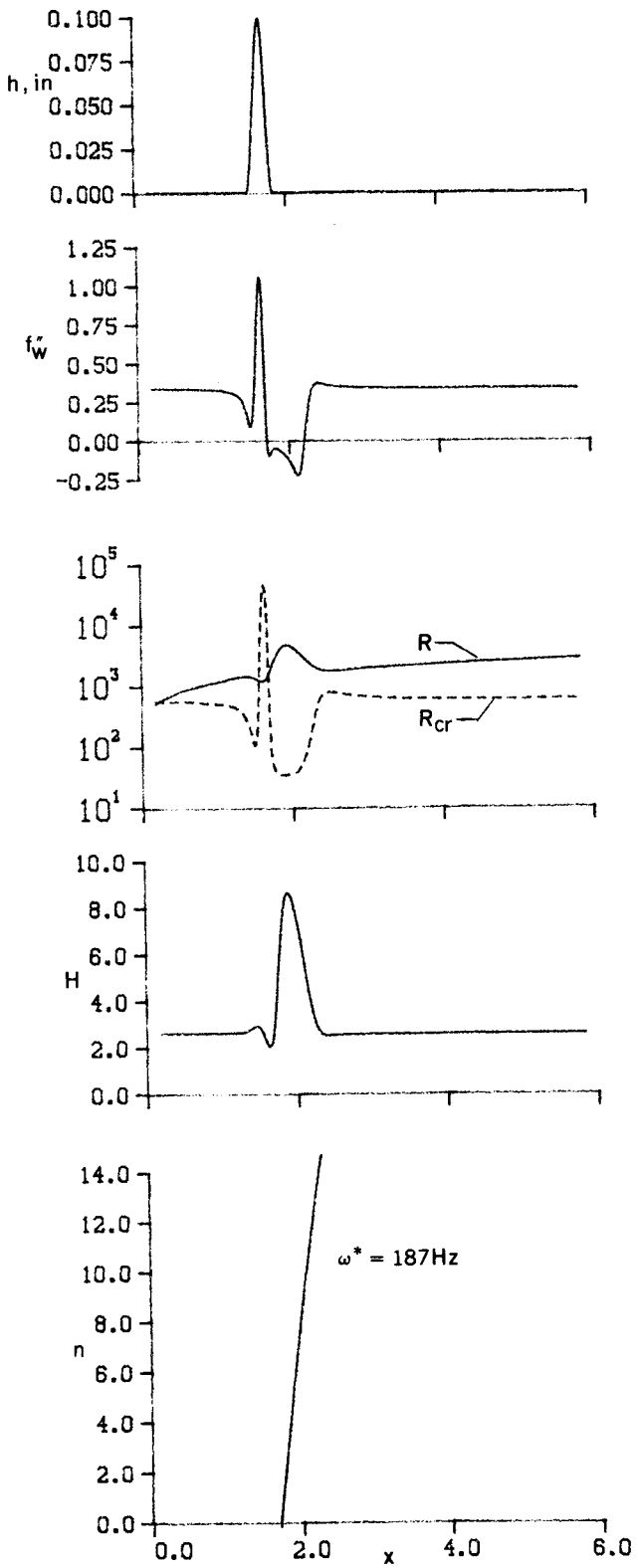

Fig. 8 Computed results for $h = 0.10$ in.

VI. Concluding Remarks

The results of the previous two sections show that a combination of an interactive boundary-layer procedure and the e^n-method leads to values of the location of the onset of transition that have trends similar to those of experimental observations. There is a tendency to predict the transition location upstream of the measured location, and this is due to a combination of uncertainties including that associated with a favorable pressure gradient in the experiments of Fage. It is clear that further work is necessary to determine the extent of improvements that can be achieved by better representation of the separated flow and by performing calculations that take into account the effects of regions of turbulent flow.

The results have shown the need for care in the evaluation of the critical frequency used in the e^n-method. In particular, fine-grid calculations were essential in the region of strong adverse pressure gradient where amplification rates were highest. For the flows considered, the choice of the location of the initial disturbance was not important provided it did not occur in the region where the critical Reynolds number was higher than the flow Reynolds number.

In some contrast to the closely related work of Nayfeh et al., the present results suggest that the e^n-method works satisfactorily for flows with separation.

Acknowledgment

This research was supported under the National Science Foundation Grant MEA 8056237.

References

[1]Holmes, B. J., Obara, C. J., and Yip, L. P., "Natural Laminar Flow Flight Experiments on Modern Airplane Surfaces," NASA TP-2256, June 1984.

[2]Holmes, B. J., Obara, C. J., Martin, G. L., and Domack, C. S., "Manufacturing Tolerances for Natural Laminar Flow Airframe Surfaces," Society of Automotive Engineers, Warrendale, PA, SAE Paper 850865, 1985.

[3]Gaster, M., "The Structure and Behavior of Laminar Separation Bubbles," AGARD CP-4, May 1966, pp. 819–854.

[4]Fage, A., "The Smallest Size of Spanwise Surface Corrugation which Affects Boundary-Layer Transition on an Airfoil," Aeronautical Research Council, R&M 2120, Jan. 1943.

[5]Carmichael, B. H., Whites, R. C., and Pfenninger, W., "Low Drag Boundary-Layer Suction Experiments in Flight on the Wing Glove of an F-94A Airplane," Northrup Corp., Rept. NAI-57-1163 (BLC-101), Aug. 1957.

[6]Carmichael, B. H., "Surface Waviness Criteria for Swept and Unswept Laminar Suction Wings," Northrup Corp., Rept. NOR-59-438 (BLC-123), Aug. 1959.

[7]Carmichael, B. H. and Pfenninger, W., "Surface Imperfection Experiments on a Swept Laminar Suction Wing," Northrup Corp., Rept. NOR-590454 (BLC-124), Aug. 1959.

[8]Smith, A. M. O., "Transition, Pressure Gradient and Stability Theory," *Proceedings of the IXth International Congress on Applied Mechanics,* Brussels, Vol. 4, 1956, pp. 234–244.

[9]Van Ingen, J. L., "A Suggested Semi-Empirical Method for the Calculation of the Boundary-Layer Transition Region," Delft, Holland, Rept. VTH74, 1956.

[10]Wazzan, A. R., "Spatial Stability of Tollmien-Schlichting Waves," *Progress in Aerospace Sciences,* Vol. 16, No. 2, Pergamon, New York, 1975, pp. 99–127.

[11]Nayfeh, A. H., Ragab, S. A., and Al-Maaitah, A., "Effect of Roughness on the Stability of Boundary Layers," AIAA Paper 86-1044, 1986.

[12]Cebeci, T., Clark, R. W., Chang, K. C., Halsey, N. D., and Lee, K., "Airfoils with Separation and the Resulting Wakes," *Journal of Fluid Mechanics,* Vol. 163, 1986, pp. 323–347.

[13]Cebeci, T., Khattab, A. A., and Schimke, S. M., "Separation and Reattachment Near the Leading Edge of an Oscillating Airfoil," *Journal of Fluid Mechanics,* Vol. 191, 1988, pp. 47–77.

[14]Cebeci, T., Kaups, K., and Khattab, A. A., "Separation and Reattachment Near the Leading Edge of a Thin Wing," *IUTAM Proceedings,* London, Aug. 1986.

[15]Veldman, A. E. P., "New Quasi-Simultaneous Method to Calculate Interacting Boundary Layers," *AIAA Journal,* Vol. 19, 1981, p. 769.

[16]Stewartson, K., "Multistructured Boundary Layers on Flat Plates and Related Bodies," *Advanced Applied Mechanics,* Vol. 14, 1974, p. 145.

[17]Cebeci, T. and Bradshaw, P., *Momentum Transfer in Boundary Layers,* Hemisphere, Washington, DC, 1977.

[18]Wang, G. S., "Stability and Transition of Similar Laminar Boundary Layers with Separation," M.S. Thesis, Dept. of Mechanical Engineering, California State Univ., Long Beach, CA, Dec. 1986.

[19]Cebeci, T., "Numerical Instabilities in the Calculation of Laminar Separation Bubbles and Their Implications," *AIAA Journal* (submitted for publication).

[20]Schubauer, G. B. and Klebanoff, P. S., "Contributions on the Mechanics of Boundary-Layer Transition," NACA TN-3489, 1955.